

HIGHLIGHTS

A method to enhance the response of rhodamine-based probes has been developed.

Fluorescence signal is enhanced by FRET inside light-harvesting nanoparticles.

100-fold decrease in LOD of Cu^{2+} probe has been demonstrated.

FRET Pumping of Rhodamine-Based Probe in Light-Harvesting Nanoparticles for Highly Sensitive Detection of Cu²⁺

A.Yu. Mironenko^{a*}, M.V. Tutov^{a,b}, A.K. Chepak^a, S.Yu. Bratskaya^a

^a – Institute of Chemistry Far Eastern Branch of the Russian Academy of Sciences, 159, prosp.100-letiya Vladivostoka, Vladivostok 690022, Russia Vladivostok, Russia

^b – Far Eastern Federal University, 8, Sukhanova St., Vladivostok 690950, Russia

* - Corresponding author. E-mail: almironenko@gmail.com

ABSTRACT

In this work we presented novel strategy for increasing the performance of popular fluorescent probes on the basis of rhodamine-lactam platform. This strategy is based on the incorporation of probe molecules into the light-harvesting nanoparticles to pump modulated optical signal by Förster resonant energy transfer. Using the commercially available Cu²⁺ probe as a reference chemical, we have developed an efficient approach to significantly improve its sensing performance. Within obtained nanoparticles coumarin-30 nanoantenna absorbs excitation light and pumps incorporated sensing molecules providing bright fluorescence to a small number of emitters, while changing the probe-analyte equilibrium from liquid-liquid to solid-liquid significantly increased the apparent association constant, which together provided a ~100-fold decrease in the detection limit. The developed nanoprobe allows highly sensitive detection of Cu²⁺ ions in aqueous media without organic co-solvents usually required for dissolution of the probe, and demonstrate compatibility with inexpensive fluorometers and the ability to detect low concentrations with the naked eye.

Keywords: fluorescent nanoprobe; Cu; sensing; FRET

1. Introduction

1 In recent years, colorimetric and fluorescent probes have become an effective
2 analytical tool due to unique capability for sensitive monitoring of metal ions [1,2],
3 anions [3,4], reactive oxygen species [5,6] and biomolecules [7,8]. Among the
4 various chromophore scaffolds, lactam derivatives of rhodamines represent one of
5 the most developed platform for the design of selective colorimetric and fluorescent
6 probes due to their high extinction coefficients, high quantum yields, and excellent
7 chemical and photostability [9,10]. Typically, such probes are rhodamine dyes
8 modified with a selective receptor capable of interacting with the analyte. The
9 sensing mechanism is based on the structural change of a molecule from a
10 spirocyclic lactam to an open-ring amide [9,10]. Without analyte the probe exists in
11 a colorless non-emissive spirocyclic form, while interaction of ligand group with
12 specific molecule or ion results in ring opening and appearance of fluorescence and
13 pink coloration.

14 Obviously, the sensitivity of analyte determination depends on the brightness of the
15 probe (absorptivity x fluorescence quantum yield), as well as the equilibrium
16 constant of probe-analyte interaction. The molar absorptivity of rhodamine 6G is
17 approximately 10^5 , and in a standard cuvette with an optical path of 10 mm, a
18 change in [probe-analyte] complex concentration of 10 nM will correspond to
19 change in optical density of ~ 0.001 , which is equal to the measurement error of a
20 typical spectrophotometer. The binding constants of real probes are in the range 10^3 -
21 10^5 , and the typical working range of analyte detection is $\sim 1\mu\text{M}$ - 0.1mM . Of course,
22 fluorescence measurements are more accurate than colorimetric, but they do not
23 provide a significant increase in sensitivity, since they have exactly the same
24 fundamental limitations. Modern approaches for ultrasensitive chemical sensing on
25 the basis of surface-enhanced Raman scattering [11–14] or surface-enhanced
26 fluorescence [15–18], allow determination of significantly lower analyte
27 concentrations, but require powerful and expensive experimental equipment, both
28 for measurements and for fabrication of nanostructured enhancing substrates.

1 It is clear that to improve the performance of fluorescent probes, it is necessary to
2 significantly enhance the response signal by pumping the probe with a much brighter
3 luminescent nanoparticle via Förster resonance energy transfer (FRET), however,
4 nanoparticles are generally not efficient FRET donors because their sizes are beyond
5 the FRET radius (1-10 nm), and in case of semiconductor nanocrystal quantum dots,
6 10–50 acceptor molecules are required to ensure efficient FRET [7]. New
7 possibilities appeared with recently introduced light-harvesting FRET nanoparticles
8 on the basis of cationic dyes separated by bulky hydrophobic counterions that
9 prevent dye self-quenching [19–22]. In these NPs a short inter-fluorophore distance
10 controlled by the counterion enable ultrafast dye–dye excitation energy migration
11 on a femtosecond time scale through the whole particle within the fluorescence
12 lifetime until it reaches a donor close to the acceptor leading to FRET. Therefore,
13 the energy can be transferred beyond Förster radius from multiple donors to a single
14 acceptor, providing a basis for signal amplification [7].

15 Inspired by recent works on the topic demonstrating the capabilities of this method,
16 we aimed to enhance the response signal of popular rhodamine-based probes. Using
17 the commercially available Cu^{2+} probe as a reference chemical, we have developed
18 an efficient approach to significantly improve its sensing performance, which
19 requires chemical modification of the probe and incorporation it into light-
20 harvesting FRET nanoparticles to amplify its fluorescence signal.

21 Within these particles coumarin 30 nanoantenna absorbs excitation light and pumps
22 incorporated sensing molecules providing bright fluorescence to a small number of
23 emitters, while changing the probe-analyte equilibrium from liquid-liquid to solid-
24 liquid significantly increased the apparent association constant, which together
25 provided a ~100-fold decrease in the detection limit. The developed nanoprobe
26 allows highly sensitive detection of Cu^{2+} ions in aqueous media without organic co-
27 solvents usually required for dissolution of the probe, and demonstrate compatibility
28 with inexpensive fluorimeters and the ability to detect low concentrations with the
29 naked eye.

2. Materials and Methods

Chemicals and instruments

Rodamine 6G (99%), Coumarin 30 (99%), 4-(dimethylamino)benzaldehyde (99%), hexane (95%), chloroform (99%), ethyl acetate (99.8%), N₂H₄*H₂O (98%), sodium tetrakis[3,5-bis(trifluoromethyl)phenyl]borate, sodium tetrakis[3,5-bis(1,1,1,3,3,3-hexafluoro-2-methoxy-2-propyl)phenyl]borate trihydrate, silica gel (100/200 μm) were purchased from Sigma-Aldrich and used as received. All other reagents were of analytical grade and used without purification. All aqueous solutions were prepared using deionized water.

The Fourier transform infrared radiation (FT-IR) spectra of the compounds in the range 400-4000 cm⁻¹ were recorded using a Perkin Elmer Spectrum 100BX II spectrometer in KBr pellets. ¹H, ¹³C NMR spectra were performed on a Bruker Avance 400 with the frequency of proton resonance 400 MHz using CDCl₃ as the solvent and tetramethylsilane as the internal reference. UV-VIS and fluorescence measurements were performed on Shimadzu UV-2600 spectrophotometer and Shimadzu RF-6000 spectrofluorophotometer using 1 cm path length cuvettes at room temperature. The size and electrokinetic potential of fluorescent particles were determined using ZetaSizer Nano ZS analyzer (Malvern Instruments Ltd.) The pH measurements were carried out using a Sartorius Professional Meter PP-50.

Synthesis and characterization of d98

Rhodamine 6G hydrazide was prepared as described in [23]. Yield 80%. ¹H NMR (400 MHz, CDCl₃, ppm, δ): 7.96 (m, 1H), 7.45 (m, 2H), 7.06 (m, 1H), 6.39 (s, 2H), 6.26 (s, 2H), 3.58 (s, 2H), 3.54 (br.s, 2H), 3.22 (q, 4H), 1.92 (s, 6H), 1.32 (t, 6H); Elemental Analysis data: Calc. C, 72.87; H, 6.59; N, 13.07; Expt. C, 72.97; H, 6.66; N, 12.89.

d98. A 300 mg (7E-4 mol) of rhodamine 6G hydrazide and 220 mg (1.4E-3 mol) of 4-(dimethylamino)benzaldehyde were dissolved in 15 ml of ethanol (95%). The mixture was refluxed for 6 h. The solvent was removed under reduced pressure and the crude product was purified by flash column chromatography on a silica gel with

1 hexane/ethylacetate (v/v = 2/1) as the eluent to afford the product as a crystal powder
2 (290 mg, 74%). ¹H NMR (400 MHz, CDCl₃, ppm, δ): 8.33 (s, 1H, H(24)), 8.03-8.04
3 (m, 1H, H(12)), 7.06-7.08 (m, 1H, H(9)), 7.45 (s, 1H, H(18)), 7.47 (s, 1H, H(19)),
4 7.61 (s, 1H, H(15)), 7.59 (s, 1H, H(22)), 7.47-7.49 (m, 2H, H(10), H(11)), 6.42 (br.
5 s, 2H, H(26), H(30)), 6.40 (br. s, 2H, H(27), H(29)), 3.50 (br.s, 2H, H(33), H(36)),
6 3.21-3.26 (q, 4H, H(34), H(37)), 2.96 (s, 6H, H(41), H(42)), 1.89 (s, 6H, H(32),
7 H(39)), 1.34-1.36 (t, 6H, H(35), H(38)); Elemental Analysis data: Calc. C, 75.11; H,
8 6.66; N, 12.51; Expt. C, 75.43; H, 6.70; N, 12.42. (¹H NMR spectrum presented in
9 Fig. S1)
10
11
12
13
14
15
16
17
18
19

20 *Preparation of fluorescent NPs*

21 1 mM of coumarin 30 in CH₃CN, 0.2mM of rhodamine 6G and d98 in CH₃CN and
22 5mM of fluorinated tetraphenylborates (sodium tetrakis[3,5-
23 bis(trifluoromethyl)phenyl]borate and sodium tetrakis[3,5-bis(1,1,1,3,3,3-
24 hexafluoro-2-methoxy-2-propyl)phenyl]borate) in CH₃CN were used as stock
25 solutions. Typically, 10 μl of coumarin 30, 0-10 μl of rhodamine 6g or d98 and 2-
26 160 μl of fluorinated tetraphenylborate stock solutions were mixed in plastic vial
27 and quickly added to 5 ml of water (1mM sodium acetate buffer, pH=5) under
28 intense stirring to yield colloidal solution of fluorescent NPs. The resulting colloidal
29 solutions were allowed to equilibrate for 60 min before use.
30
31
32
33
34
35
36
37
38
39
40
41
42
43
44
45
46
47
48
49
50
51
52
53
54
55
56
57
58
59
60
61
62
63
64
65

3. Results and discussion.

1 In the ion association method for preparation of fluorescent nanoparticles, a
2 hydrophobic cation and anion, dissolved in water, are mixed together to form
3 insoluble salts, which are precipitated in the form of nanoparticles consisting of a
4 large number of fluorescent ions separated by counterions [21]. It has recently been
5 shown that the use of bulky hydrophobic anions can significantly reduce aggregation
6 of cationic dyes and minimize the effects of aggregation induced fluorescence
7 quenching. Moreover, incorporated dye molecules are strongly coupled by energy
8 transfer and can be very efficient energy donors in light-harvesting FRET systems
9 [7,21,24,25].

10
11
12
13
14
15
16
17
18
19
20 A. Klymchenko group have published a series of papers on light harvesting FRET
21 nanoparticles where rhodamine B emitting at ~580 nm was used as donor to pump
22 near-IR emitting acceptor [7,21,24,25]. Here we targeted on pumping rhodamine 6g,
23 what require green-emitting (500-550 nm) cationic dye with high fluorescence
24 quantum yield (FLQY). The search for a suitable energy donor among commercially
25 available laser dyes has shown that only anionic (fluoresceins) and neutral
26 (coumarins) dyes have the required spectral properties. We hypothesized that neutral
27 molecules containing amino groups (amines), capable for protonation (i.e., the
28 formation of a positively charged ammonium ion) will also associate with
29 hydrophobic counterions since chemical equilibrium is always shifted toward
30 formation of insoluble products. Taking into account molecular structure and
31 spectral properties we used coumarin 30 (C30) as donor, rhodamine 6g (R6G) as
32 acceptor and fluorinated tetraphenylborates (f-TPB) as counterions (the used
33 chemicals presented in Fig. 1).
34
35
36
37
38
39
40
41
42
43
44
45
46
47
48
49
50
51
52
53
54
55
56
57
58
59
60
61
62
63
64
65

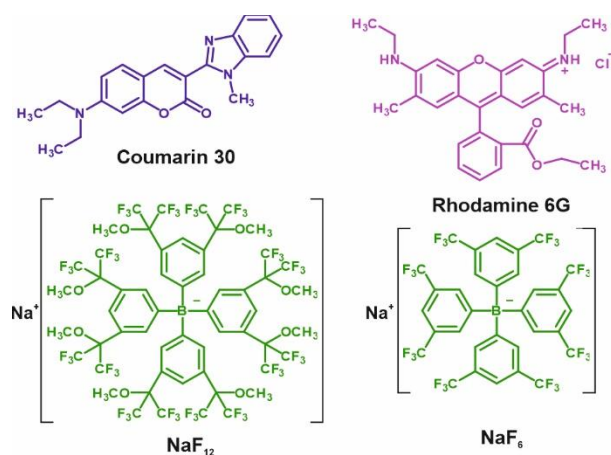


Fig. 1 Chemical structures of the coumarin 30, rhodamine 6G and fluorinated tetraphenylborates used in this work.

To avoid any problems associated with poor water solubility of raw materials, the synthesis of C30/f-TPB nanoparticles was based on nanoprecipitation from the water-miscible solvent: the dye and corresponding f-TPB were dissolved in small volume of acetonitrile in required ratio and quickly added to water under intense stirring to yield C30/f-TPB colloidal solution. Preliminary experiments have shown that with a sufficient excess of f-TPB, ion association occurs throughout all tested pH range (2-10), however fluorescence of acidic solutions was higher than that of basic ones. Since the work was focused on improving the performance of the rhodamine-lactam platform, all further experiments were performed at pH = 5, the maximally acidic environment in which the response of such probes is not cross-influenced by hydrogen ions [26].

In the search for the optimal C30/counterion ratio, which ensures the stability of resulting colloidal solution and a high FLQY, we varied the excess of the counterion at a fixed dye concentration. Fig. 2(a, c, d) shows that with a sufficient excess of corresponding f-TPB, the absorbance of the resulting solution is significantly higher than that of coumarin aqueous solution of the same concentration, while the absorption band is red-shifted (Fig. 2a, solid curves). This spectral shift clearly indicates protonation of coumarin and redistribution of electronic density, which was also confirmed by acidification of the coumarin with hydrochloric acid, where a similar redshift was observed (Fig. 2a, dashed curves). In the case of an equimolar

1 ratio or a slight excess of the counterion (less than 5), the resulting solutions are
2 much less stable and partially precipitate within a few hours, while at higher
3 counterion concentration the solutions remained stable for at least several weeks.
4 DLS measurements (Fig. 2(c, d), blue curves) revealed that the size of the formed
5 particles also changes with an increase in counterion excess. In the case of F12, the
6 size sequentially decreases from 140 to 30 nm at a 20-fold excess and remains
7 unchanged (Fig. 2c, blue curve), while in the case of F6 it gradually increases from
8 60 to 100 nm (Fig 2d, blue curve). This difference can be explained by difference in
9 solubility of corresponding anion precursors. Thus, NaF12 is soluble in water, the
10 resulting NPs mainly consist of the insoluble salt C30/F12, while the excess of
11 anions is adsorbed on solid surface, forming the first negatively charged layer of the
12 electric double layer (more anions stabilize smaller particles). The solubility of NaF6
13 in water is much lower and it coprecipitate with C30/F6 forming large mixed
14 particles. It is noteworthy that in both cases a higher excess of counterions provides
15 the dye a higher FLQY (Fig. 2(c, d)): at pH=5, the maximum quantum yields were
16 ~ 40% and 20% for F12 and F6, respectively, whereas in an aqueous solution without
17 counterions, FLQY of coumarin was 0.08 at pH=7 and 0.04 at pH=5 (for
18 comparison, in EtOH, FLQY=0.8). A similar impressive fluorescence light up has
19 been noted for rhodamine B, a cationic dye, and was attributed to unique
20 hydrophobic environment within the nanoparticles [21], however, for a neutral dye
21 that is quenched upon protonation even in good solvent (Fig. S2), this is the first-
22 time report.
23
24
25
26
27
28
29
30
31
32
33
34
35
36
37
38
39
40
41
42
43
44
45
46
47
48
49
50
51
52
53
54
55
56
57
58
59
60
61
62
63
64
65

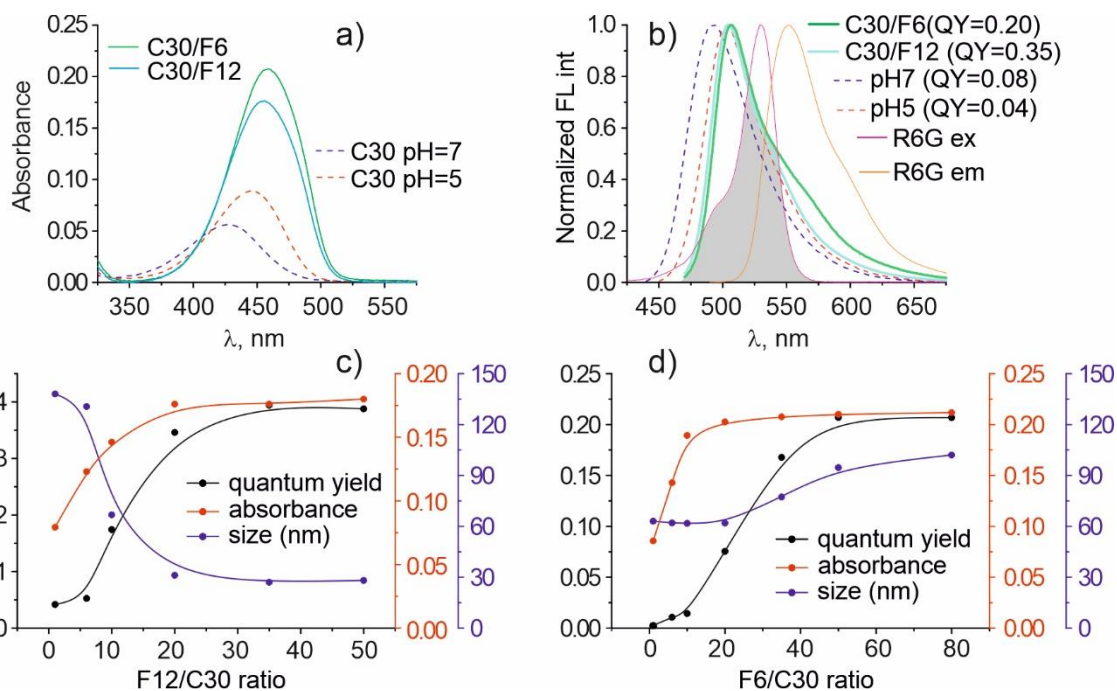


Fig. 2 Characterization of coumarin 30/f-TPB nanoparticles. a) absorbance spectra of C30/F6 (1/20, mol/mol), C30/F12 (1/50, mol/mol), and coumarin 30 aqueous solution at pH=7 and pH=5. b) emission spectra of C30/F6, C30/F12, coumarin 30 and excitation and emission spectra of R6G (spectral overlap of C30/F6 emission and R6G excitation is marked in gray; FLQY is given in the legend). The change in absorbance at $\lambda_{max} = 460\text{nm}$, FLQY and average particle size of synthesized C30/F12 (c) and C30/F6 (d) nanoparticles on the counterion excess.

We then obtained FRET nanoparticles with the fixed C30/counterion ratios (C30/F6=1/50, C30/F12=1/20) and a variable amount of the model acceptor (R6G) in order to estimate the donor/acceptor ratio, ensuring a noticeable energy transfer within nanoparticles. As shown in Fig. 3(a, b, d, e) Incorporation of R6G molecules into NPs leads to the appearance of a new emission band at $\sim 540\text{-}550\text{ nm}$ with a decrease in the characteristic emission band of coumarin, indicating the occurrence of FRET. Fig. 3c shows that smaller F12-based NPs are better energy donors than F6-based NPs: 4.8 and 6.2 acceptor molecules per 100 donors are required for 50% FRET efficiency in F12- and F6-based NPs, respectively. It should also be noted that with an increase in acceptor loading, FLQY of obtained NPs slightly increases (Fig. 3f) and reaches maximum at a ratio of R6G/C30 = 1/10. Thus, taking into account

FLQY and FRET efficiency, we have established optimal composition of fret nanoparticles ($C30/R6G/F12 = 1/10/20$ and $C30/R6G/F6 = 1/10/50$) for the further development of the sensitive probe.

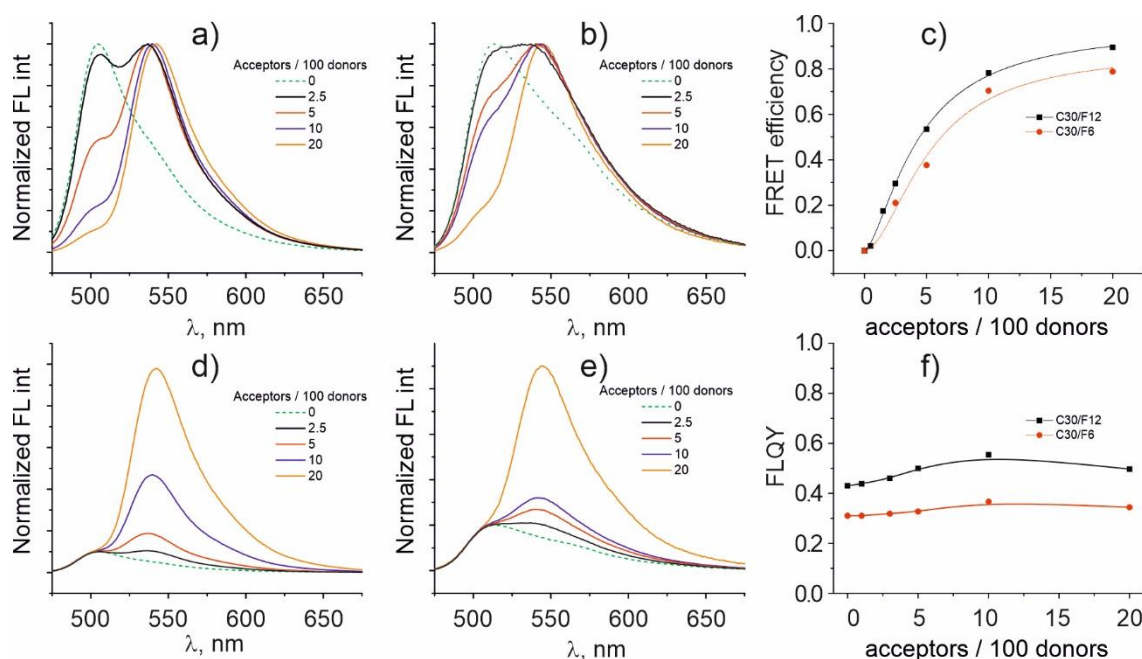


Fig. 3 Characterization of C30/R6G/f-TPB FRET NPs. Normalized to unity and to donor emission fluorescence spectra of C30/R6G/F12 (a, d) and C30/R6G/F5 (b, e) FRET nanoparticles. Dependence of FRET efficiency (c) and FLQY (f) of FRET NPs on acceptor loading.

The platform based on lactam derivatives of rhodamine is probably the most popular for the development of selective cation sensors. Its general principle is shown in the Fig. S3. Rhodamine lactams are colorless, non-fluorescent materials with pH-dependent halochromic properties. When N atom of lactam ring modified with appropriate receptor, the optical response can be induced by specific analyte at fixed pH level. Obviously, typical probes will not work inside the obtained NPs, since, as has been shown, ionic association with F6 and F12 leads to protonation of amines even in an alkaline medium, and, thus, the sensor molecule will be "switched on" without analyte. To get around this limitation, we synthesized a new derivative d98, which is rhodamine 6G hydrazide (a commercially available probe for the determination of Cu^{2+}), modified with an electron-donating amino aromatic group, which is introduced to change optical response of the probe via photoinduced

electron transfer (PET) fluorescence quenching. Brief description of this mechanism is presented in Fig. 4.

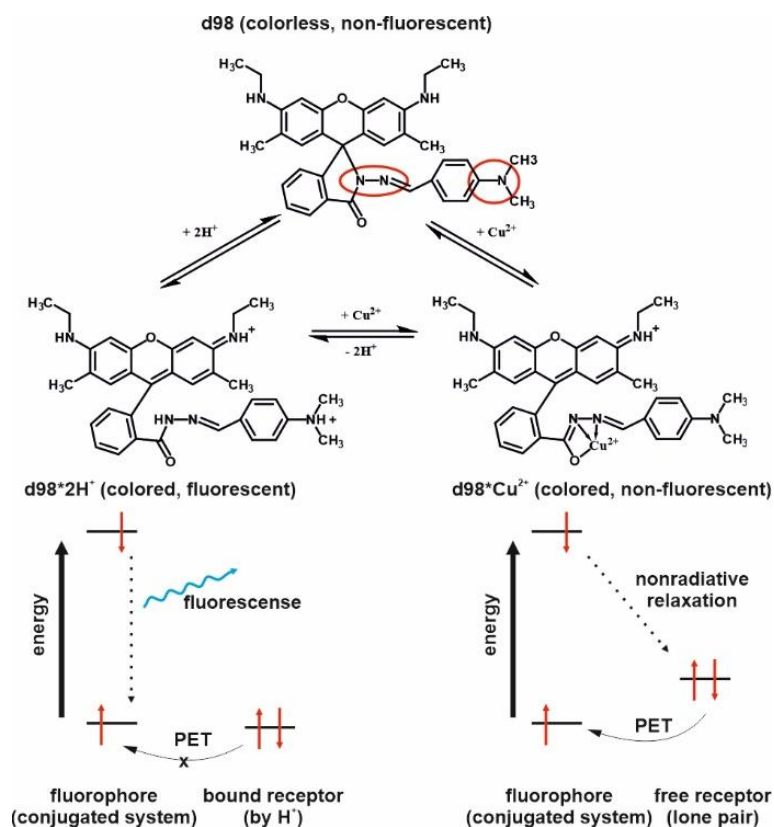


Fig. 4. Schematic representation of the optical response of d98 upon binding H⁺ and Cu²⁺ ions.

d98 has 2 binding sites - hydrazone and aminoaromatic fragments (marked with red circles in Fig. 4). The hydrazone fragment has affinity for both Cu²⁺ and H⁺, while the aminoaromatic one only for H⁺. In an acidic medium, both sites are occupied and d98 is colored and fluorescent, while in the presence of Cu²⁺ only the hydrazone fragment is occupied, and d98 is colored and non-fluorescent. In a moderately acidic medium, the copper ion displaces both protons from the molecule, and thus its concentration can be determined from the change in the fluorescence intensity of the solution at constant absorption (i.e., by decrease in FLQY).

To test whether a similar effect will take place inside the nanoparticles, light-harvesting nanoprobe were synthesized with an optimized ratio of precursors C30/d98/F6 = 10/1/500 and C30/d98/F12 = 10/1/200. It should be pointed out that coumarin 30, like many other amines, can coordinate copper ions with a change in

1 optical properties; therefore, we studied the optical response of all new materials
2 presented in the work: d98 in a water/ethanol (50/50, v/v), coumarin NPs, and FRET
3 NPs with R6G and d98 acceptors. The data presented in Fig. 5(a, b) show that
4 quenching of C30 and C30/R6G NPs proceeds in exactly the same way, while
5 C30/d98 NPs demonstrate essentially shifted to lower concentrations response
6 curves, what can be interpreted as quenching of the same number of emitters with a
7 smaller amount of analyte. It is noteworthy that Cu^{2+} binding affects only the
8 quantum yield, while the absorption spectra, particle size and zeta potential remain
9 the same. To confirm that observed quenching is a result of d98- Cu^{2+} interaction, we
10 analyzed the stoichiometry of binding event according to Job's method. Fig. 5c
11 clearly demonstrate 1:1 binding stoichiometry between d98 and Cu^{2+} both in the case
12 of d98 solution and in the case of NPs containing d98. All these data reliably confirm
13 the successful implementation of the key idea of the work: to increase the
14 performance of the probe by pumping it with multiple donor molecules; however,
15 the achieved increase in performance turned out to be much higher than the optical
16 pumping factor. We believe that such behavior is associated with a change in the
17 type of chemical equilibrium. Fluorescent probes are usually poorly soluble in water
18 and require organic co-solvent, which provides the probe solubility and reversible
19 probe-complex equilibrium in homogeneous solution. In our case, solid
20 nanoparticles act as a cation exchanger; thus, the observed response is the result of
21 a heterogeneous sorption process with much higher equilibrium constant. F6- and
22 F12-based NPs provide 10- and 100-fold better sensitivity than d98 in solution.
23 Finally, interference experiments to study the effect of other ions on sensing
24 performance were performed for C30/d98/F12 sample. Fig.5(d) presents the
25 response of the probe on the presence of 10^{-5} M Cu^{2+} with tenfold excess of tested
26 cation. The results show that developed nanoprobe is suitable for selective detection
27 of Cu^{2+} in the presence of a wide range of environmentally relevant ions and can
28 serve as a naked-eye sensor.
29
30
31
32
33
34
35
36
37
38
39
40
41
42
43
44
45
46
47
48
49
50
51
52
53
54
55
56
57
58
59
60
61
62
63
64
65

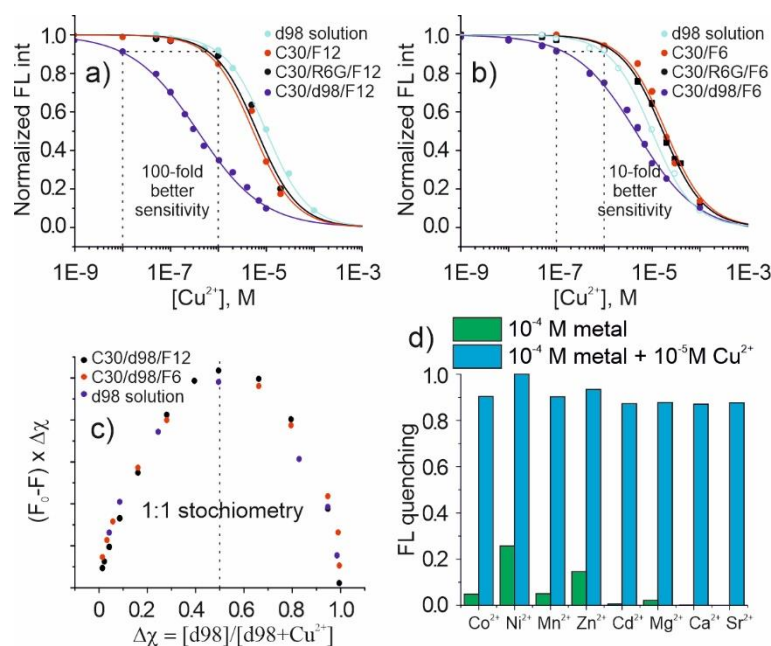


Fig. 5. Dependence of response signal on the analyte concentration for C30/F12, C30/R6G/F12, C30/d98/F12 NPs (a) and C30/F6, C30/RG/F6, C30/d98/F12 NPs (b). Job's plots (method of continuous variation) showing formation 1:1 Cu:d98 complexes in solution and inside NPs. Influence of interfering metal ions (10^{-4} M) on response value of C30/d98/F12 nanoprobe to the presence of 10^{-5} M Cu^{2+} (d).

4. Conclusions

To conclude, we have presented novel strategy for increasing the performance of very popular fluorescent rhodamine probes, which is based on the incorporation of probe molecules into the light-harvesting nanoparticles to pump optical signal by Förster resonant energy transfer.

According to published works, for the formation of bright FRET particles (without aggregation caused quenching), cationic dyes should be associated with bulky hydrophobic anions, however, organic cationic dyes emit in the yellow-NIR spectral range, which means that the blue-green absorbing dyes can be used only as donors, but not as acceptors. We have shown that neutral dyes containing amino groups act as cationic dyes and can also be used in the ion association method for preparation of fluorescent nanoparticles to pump blue-green absorbing cationic dyes.

Finally, on the basis of commercially available Cu^{2+} probe we have developed FRET-nanoprobe with sub-nM detection limit which demonstrate compatibility with

1 inexpensive fluorimeters and the ability to detect low concentrations of Cu²⁺ with
2 the naked eye.
3
4

5 **Acknowledgements**

6
7 This work was financially supported by the Russian Foundation of Basic Research,
8 project number 20-53-76016 ERA_t within a cooperative project RUS_ST2019-245
9 EMPOLSENS of the ERA-Net RUS Plus Program of the European Commission.
10
11
12
13
14

15 **References**

- 16
17 [1] Tutov MV, Sergeev AA, Zadorozhny PA, Bratskaya SY, Mironenko AY.
18 Dendrimeric rhodamine based fluorescent probe for selective detection of
19 Au. *Sensors Actuators, B Chem* 2018;273:916–20.
20 <https://doi.org/10.1016/j.snb.2018.05.117>.
21
22 [2] Mironenko AY, Tutov MV, Sergeev AA, Voznesenskiy, Bratskaya SY.
23 On/off rhodamine based fluorescent probe for detection of Au and Pd in
24 aqueous solutions. *Sensors Actuators, B Chem* 2017;246:389–94.
25 <https://doi.org/10.1016/j.snb.2017.02.092>.
26
27 [3] Wang L, Ding H, Ran X, Tang H, Cao D. Recent progress on reaction-based
28 BODIPY probes for anion detection. *Dye Pigment* 2020;172:107857.
29 <https://doi.org/10.1016/J.DYEPIG.2019.107857>.
30
31 [4] La M, Hao Y, Wang Z, Han GC, Qu L. Selective and Sensitive Detection of
32 Cyanide Based on the Displacement Strategy Using a Water-Soluble
33 Fluorescent Probe. *J Anal Methods Chem* 2016;2016.
34 <https://doi.org/10.1155/2016/1462013>.
35
36 [5] Wu L, Sedgwick AC, Sun X, Bull SD, He X-P, James TD. Reaction-Based
37 Fluorescent Probes for the Detection and Imaging of Reactive Oxygen,
38 Nitrogen, and Sulfur Species. *Acc Chem Res* 2019;52:2582–97.
39 <https://doi.org/10.1021/ACS.ACCOUNTS.9B00302>.
40
41 [6] Nguyen VN, Ha J, Cho M, Li H, Swamy KMK, Yoon J. Recent
42 developments of BODIPY-based colorimetric and fluorescent probes for the
43
44
45
46
47
48
49
50
51
52
53
54
55
56
57
58
59
60
61
62
63
64
65

- 1
2
3
4
5
6
7
8
9
10
11
12
13
14
15
16
17
18
19
20
21
22
23
24
25
26
27
28
29
30
31
32
33
34
35
36
37
38
39
40
41
42
43
44
45
46
47
48
49
50
51
52
53
54
55
56
57
58
59
60
61
62
63
64
65
- detection of reactive oxygen/nitrogen species and cancer diagnosis. *Coord Chem Rev* 2021;439:213936. <https://doi.org/10.1016/J.CCR.2021.213936>.
- [7] Melnychuk N, Egloff S, Runser A, Reisch A, Klymchenko AS. Light-Harvesting Nanoparticle Probes for FRET-Based Detection of Oligonucleotides with Single-Molecule Sensitivity. *Angew Chemie Int Ed* 2020;59:6811–8. <https://doi.org/10.1002/ANIE.201913804>.
- [8] Jurek K, Kabatc J, Kostrzevska K, Grabowska M. New Fluorescence Probes for Biomolecules. *Mol* 2015, Vol 20, Pages 13071-13079 2015;20:13071–9. <https://doi.org/10.3390/MOLECULES200713071>.
- [9] Kim HN, Lee MH, Kim HJ, Kim JS, Yoon J. A new trend in rhodamine-based chemosensors: application of spirolactam ring-opening to sensing ions. *Chem Soc Rev* 2008;37:1465. <https://doi.org/10.1039/b802497a>.
- [10] Chen X, Pradhan T, Wang F, Kim JS, Yoon J. Fluorescent Chemosensors Based on Spiroring-Opening of Xanthenes and Related Derivatives. *Chem Rev* 2011;112:1910–56. <https://doi.org/10.1021/CR200201Z>.
- [11] Mitsai E, Kuchmizhak A, Pustovalov E, Sergeev A, Mironenko A, Bratskaya S, et al. Chemically non-perturbing SERS detection of a catalytic reaction with black silicon. *Nanoscale* 2018;10:9780–7. <https://doi.org/10.1039/c8nr02123f>.
- [12] Shinde SS, Bhosale CH, Rajpure KY. Oxidative degradation of acid orange 7 using Ag-doped zinc oxide thin films. *J Photochem Photobiol B Biol* 2012;117:262–8. <https://doi.org/10.1016/j.jphotobiol.2012.10.011>.
- [13] Pavliuk G, Pavlov D, Mitsai E, Vitrik O, Mironenko A, Zakharenko A, et al. Ultrasensitive SERS-based plasmonic sensor with analyte enrichment system produced by direct laser writing. *Nanomaterials* 2020;10. <https://doi.org/10.3390/nano10010049>.
- [14] Mitsai E, Naffouti M, David T, Abbarchi M, Hassayoun L, Storozhenko D, et al. Si_{1-x}Ge_x nanoantennas with a tailored Raman response and light-to-heat conversion for advanced sensing applications. *Nanoscale* 2019;11. <https://doi.org/10.1039/c9nr01837a>.

- 1
2
3
4
5
6
7
8
9
10
11
12
13
14
15
16
17
18
19
20
21
22
23
24
25
26
27
28
29
30
31
32
33
34
35
36
37
38
39
40
41
42
43
44
45
46
47
48
49
50
51
52
53
54
55
56
57
58
59
60
61
62
63
64
65
- [15] Dostovalov A, Bronnikov K, Korolkov V, Babin S, Mitsai E, Mironenko A, et al. Hierarchical anti-reflective laser-induced periodic surface structures (LIPSSs) on amorphous Si films for sensing applications. *Nanoscale* 2020;12:13431–41. <https://doi.org/10.1039/d0nr02182b>.
- [16] Borodaenko Y, Gurbatov S, Tutov M, Zhizhchenko A, Kulinich SA, Kuchmizhak A, et al. Direct femtosecond laser fabrication of chemically functionalized ultra-black textures on silicon for sensing applications. *Nanomaterials* 2021;11. <https://doi.org/10.3390/nano11020401>.
- [17] Mironenko AY, Tutov MV, Sergeev AA, Mitsai EV, Ustinov AY, Zhizhchenko AY, et al. Ultratrace Nitroaromatic Vapor Detection via Surface-Enhanced Fluorescence on Carbazole-Terminated Black Silicon. *ACS Sensors* 2019;4:2879–84. <https://doi.org/10.1021/acssensors.9b01063>.
- [18] Sergeeva KA, Tutov MV, Voznesenskiy SS, Shamich NI, Mironenko AY, Sergeev AA. Highly-sensitive fluorescent detection of chemical compounds via photonic nanojet excitation. *Sensors Actuators, B Chem* 2020;305. <https://doi.org/10.1016/j.snb.2019.127354>.
- [19] Trofymchuk K, Reisch A, Didier P, Fras F, Gilliot P, Mely Y, et al. Giant light-harvesting nanoantenna for single-molecule detection in ambient light. *Nat Photonics* 2017;11:657–63. <https://doi.org/10.1038/s41566-017-0001-7>.
- [20] Andreiuk B, Aparin IO, Reisch A, Klymchenko AS. Bulky Barbiturates as Non-Toxic Ionic Dye Insulators for Enhanced Emission in Polymeric Nanoparticles. *Chem – A Eur J* 2021;27:12877–83. <https://doi.org/10.1002/CHEM.202101986>.
- [21] Shulov I, Oncul S, Reisch A, Arntz Y, Collot M, Mely Y, et al. Fluorinated counterion-enhanced emission of rhodamine aggregates: Ultrabright nanoparticles for bioimaging and light-harvesting. *Nanoscale* 2015;7:18198–210. <https://doi.org/10.1039/c5nr04955e>.
- [22] Aparin IO, Melnychuk N, Klymchenko AS. Ionic Aggregation-Induced Emission: Bulky Hydrophobic Counterions Light Up Dyes in Polymeric Nanoparticles. *Adv Opt Mater* 2020;8:2000027.

<https://doi.org/10.1002/ADOM.202000027>.

- 1
2
3
4
5
6
7
8
9
10
11
12
13
14
15
16
17
18
19
20
21
22
23
24
25
26
27
28
29
30
31
32
33
34
35
36
37
38
39
40
41
42
43
44
45
46
47
48
49
50
51
52
53
54
55
56
57
58
59
60
61
62
63
64
65
- [23] Zhang JF, Zhou Y, Yoon J, Kim Y, Kim SJ, Kim JS. Naphthalimide Modified Rhodamine Derivative: Ratiometric and Selective Fluorescent Sensor for Cu²⁺ Based on Two Different Approaches. *Org Lett* 2010;12:3852–5. <https://doi.org/10.1021/ol101535s>.
- [24] Trofymchuk K, Reisch A, Didier P, Fras F, Gilliot P, Mely Y, et al. Giant light-harvesting nanoantenna for single-molecule detection in ambient light. *Nat Photonics* 2017 1110 2017;11:657–63. <https://doi.org/10.1038/s41566-017-0001-7>.
- [25] Severi C, Melnychuk N, Klymchenko AS. Smartphone-assisted detection of nucleic acids by light-harvesting FRET-based nanoprobe. *Biosens Bioelectron* 2020;168:112515. <https://doi.org/10.1016/j.bios.2020.112515>.
- [26] Mironenko AY, Tutov MV, Chepak AK, Zadorozhny PA, Bratskaya SY. A novel rhodamine-based turn-on probe for fluorescent detection of Au³⁺ and colorimetric detection of Cu²⁺. *Tetrahedron* 2019;75:1492–6. <https://doi.org/10.1016/j.tet.2019.01.068>.